Geophys. J. Int. (2008) **172,** 18–30 doi: 10.1111/j.1365-246X.2007.03630.x

Isolating the PGR signal in the GRACE data: impact on mass balance estimates in Antarctica and Greenland

V. R. Barletta,[1] R. Sabadini[1] and A. Bordoni[2]

[1] *Dipartimento di Scienze della Terra 'A. Desio', Università di Milano, Italy. E-mail: valentina.barletta@unimi.it*
[2] *Dipartimento di Fisica. Università di Milano, Italy*

Accepted 2007 September 21. Received 2007 July 13; in original form 2007 January 22

SUMMARY

Redistribution of mass over the Earth and within the mantle changes the gravity field whose variations are monitored at high spatial resolution by the presently flying GRACE space gravity mission from NASA or, at longer wavelengths, by the Satellite Laser Ranging (SLR) constellation. In principle, GRACE data allow one to study the time evolution of various Earth phenomena through their gravitational effects. The correct identification of the gravitational spatial and temporal fingerprints of the individual hydrologic, atmospheric, oceanographic and solid Earth phenomena is thus extremely important, but also not trivial. In particular, it has been widely recognized that the gravitational estimates of present-day ice mass loss in Greenland and Antarctica, and the related effect on sea level changes, depend on an accurate determination of the Postglacial Rebound (PGR) after Pleistocene deglaciation, which in turn depends on the assumed solid Earth parameters and deglaciation model. Here we investigate the effect of the uncertainty of the solid Earth parameters (viscosity, litospheric thickness) and of different deglaciation processes on PGR in Greenland and Antarctica. We find that realistic constraints to the trend in ice mass loss derived from GRACE data determine a range of variation substantially wider than commonly stated, ranging from an important ice loss of -209 Gt yr^{-1} to an accumulation of $+88$ Gt yr^{-1} in Antarctica, and Greenland ablation at a rate between -122 and -50 Gt yr^{-1}. However, if we adopt the set of most probable Earth parameters, we infer a substantial mass loss in both regions, -171 ± 39 and -101 ± 22 Gt yr^{-1} for Antarctica and Greenland, respectively.

Key words: Time series analysis; Satellite geodesy; Time variable gravity; Dynamics of lithosphere and mantle; Rheology: mantle; Antarctica.

1 INTRODUCTION

The gravitational signal registered by GRACE data is due to several different sources, and the identification of the individual contributions is an essential issue in an accurate analysis.

In particular, the gravitational time-series can be seen as the sum of periodic signals, like those due to seasonal hydrologic phenomena or the periodic atmospheric and oceanographic processes, and a secular contribution, due to non-periodic modification of Earth mass distribution, like Postglacial Rebound (PGR). The latter, together with hydrological and atmospheric phenomena, is responsible for the most visible signatures in the Earth's time dependent gravity field. For example, ice sheet modifications in Earth glaciers show a seasonal variation superimposed on a trend that should depend on the global climate modification and PGR signal. Indeed, PGR reveals itself as a secular component in the gravity field, depending on mantle viscosity.

The separation of the secular trend from the periodic signal is feasible, and the accuracy of the separation improves with the availability of data spanning longer time intervals.

In this respect, while sophisticated analyses are carried on to extract the different periodic variations by comparing the GRACE gravitational data with results from, for example, atmospheric, oceanographic and hydrologic models, employing results from independent methods, the discrimination of the different secular contributions is usually made in a simplified way. In fact, most of the attention is devoted to accurately remove spurious signals due to different physical surface phenomena, or to errors (stripes) related to satellite measurements; the separation of the most important secular contribution, the PGR after the Pleistocene deglaciation, is usually oversimplified.

Results from PGR geophysical modelling and the even and odd low degree harmonics of time dependent gravity field have been used to constrain the mantle viscosity profile and present-day ice mass balance in Antarctica and Greenland (Tosi *et al.* 2005) using Satellite Laser Ranging (SLR). On the other hand, results from GRACE data analyses (Velicogna & Wahr 2005, 2006a,b; Chen *et al.* 2006a,b; Lutchke *et al.* 2006) and other sources (Ramillien *et al.* 2006; Rignot *et al.* 2006) confirm that Antarctica and Greenland are loosing ice mass.

In the present study we make use of GRACE harmonic coefficients (level 2 GRACE products from various analysis centres) in conjunction with our PGR models, in order to bound present-day ice mass balance in Antarctica and Greenland, on the basis of a thorough search in the viscosity space of PGR models. Note that most of the atmospheric and barotropic oceanic mass redistribution effects have been removed from GRACE harmonic coefficients (Bettadpur 2003).

We investigate in detail the dependence of the present-day PGR signal in Antarctica and Greenland on the physical solid Earth parameters and on deglaciation models. We show that varying the parameters in a neighbourhood of the most probable physical values obtained from inversion problems, the ice sheet mass estimates derived from GRACE data can vary in a relatively wide range. This means that the PGR contribution cannot be simply removed as a pure number from the GRACE derived trend, but it must be treated at least as accurately as all the other surface contributions.

The main aim of this work is to evaluate the variability induced by the uncertainty in PGR modelling, and by different deglaciation processes, on present-day ice variation estimates on Antarctica and Greenland, rather than to provide GRACE data based accurate estimates of the ice mass variations. Thus, in order to avoid to introduce artefacts due to sophisticated data processing, we perform a simple analysis of GRACE data, favouring instead a thorough analysis of PGR modelling.

A critical analysis of level 2 GRACE products from the three official analysis centres, namely Center for Space Research (The University of Texas at Austin: CSR), GeoForschungsZentrum (GFZ Potsdam) and Jet Propulsion Laboratory (JPL, California Institute of Technology), justifies the use of the available and most updated GFZ release 03.

2 RELIABILITY OF LEVEL 2 GRACE PRODUCTS IN THE POLAR REGIONS

GRACE level 2 data are provided by two production (CSR and GFZ) and one validation (JPL) independent analysis centres. In order to choose the most suitable time-series among the three centres, we make use of monthly mass grids evaluated by Chambers (2006). These mass grids have the advantage of being available for the three time-series (GFZ, CSR and JPL) and of taking into account the same kind of corrections such as leakage, destriping, and ocean pole tides, the latter only for the CSR release 01. In particular, the destriping corrections should reduce a systematic error in the high degree coefficient (Chambers 2006), as will be better clarified in the following.

For each of the three series and for each month we provide a rough estimate of mass variations in giga, or 10^9 tons per year (Gt yr^{-1}) over Antarctica and Greenland, and the results are shown in the two graphs in the top row of Fig. 1, where blue, red and green stand for CSR, GFZ and JPL time-series, respectively. These mass variations are evaluated by integrating the monthly mass grids over the region of interest

$$\delta\sigma_t = \int_{\text{Region}} \Delta\sigma_t(\theta, \varphi)\, \mathrm{d}\Omega, \tag{1}$$

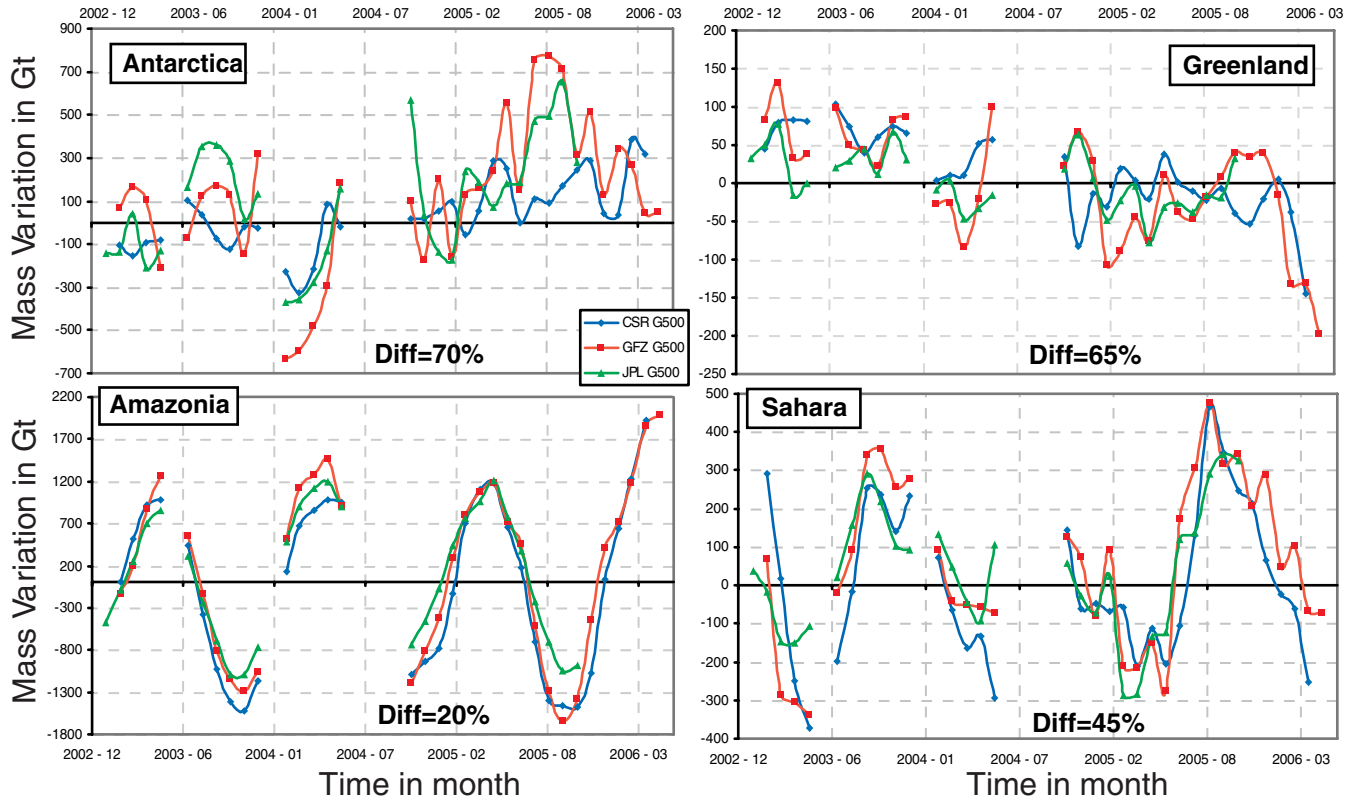

Figure 1. Monthly mass variation, in Gt, over Antartica and Greenland, top row, and Amazonia and Sahara, bottom row. Blue, red and green curves stand for CSR, GFZ and JPL time-series. Diff denotes the ratio between the mean of the variation among the three series and the amplitude over the region of interest. The equivalent Gaussian filter size is 500 km, from now on indicated in figure legend by G followed by size in km.

where $\delta\sigma_t$ denotes the mass change corresponding to the month t. $\Delta\sigma_t(\theta, \varphi)$ is the function which provides the mass grids:

$$\Delta\sigma_t(\theta,\varphi) = \frac{a\rho_E}{3}\sum_{\ell,m}\frac{2\ell+1}{k_\ell+1}\overline{P}_{\ell m}(\cos\theta) \times (C_{\ell m}(t)\cos\varphi + S_{\ell m}(t)\sin\varphi), \quad (2)$$

where $\overline{P}_{\ell m}$ are the normalized Legendre polynomials, $C_{\ell m}(t)$ and $S_{\ell m}(t)$ are the GRACE coefficients corresponding to the month t, k_ℓ are the Love numbers, a is the mean radius of the Earth, ρ_E is the average density of the Earth, according to Wahr *et al.* (1998). The colatitude is θ and the longitude is φ.

There are evident differences among the three series. Note that four months (from 2004 July to 2004 October) are missing because of deep resonance of GRACE satellites, and consequent poor resolution (Bettadpur *et al.* 2006; Chambers 2006).

Antarctica and Greenland are compared with regions such as Amazonia and Sahara where mass variabilities have certainly a different origin from that affecting the polar regions of the Earth: it is notable from the two graphs in the bottom row of Fig. 1 that over Amazonia and Sahara the relative differences among the various series are smaller. The hydrological cycle is evident in Amazonia, and perhaps over the Sahara region. It is noteworthy that the amplitude of mass variations ranges from 10^3 Gt over the Amazon basin to 10^2 Gt over Greenland.

To quantify the differences among the three series we make use of the ratio Diff between the mean of the monthly variation σ_t among the three series, and the variability of the signal in the selected region, resulting into a percentage value. Explicitly:

$$\mathrm{Diff} = \frac{\frac{1}{N}\sum_{t=1}^{N}\sigma_t}{\sigma_{\mathrm{Ave}}},$$

where σ_t is the standard deviation of the three series epoch by epoch, so the numerator is the average over the entire period. The denominator, σ_{Ave} is the standard deviation, over the entire period, of a series which is the average, epoch by epoch, of the three series. Of course, if the signal has a strong trend, σ_{Ave} is time-dependent, and it grows with time. So this simple analysis, for those kind of signal, underestimates the ratio Diff, as for Antarctica and Greenland which show a strong trend, and yet the differences are evident compared to Amazonia and Sahara.

The parameter Diff varies from 70 and 65 per cent for Antarctica and Greenland to 20 and 45 per cent for Amazonia and Sahara, thus differences are larger in the polar regions, which makes the choice of the time-series critical for mass change estimates over these regions.

CSR 01 products need some corrections, for example the pole tide, which has been included in release 2. The GFZ R03 data provide meaningful results over land only if the atmospheric–oceanic model (GAB) is accounted for, as recommended in the release notes of the time-series (Bettadpur *et al.* 2006): these corrections have a large impact mostly on the polar regions. Chambers (2006) shows that the latest available time-series (CSR 02, GFZ 03, JPL 02) are improved with respect to the previous ones, that are of very similar accuracy and suggests that the mean of the three time-series is the optimal choice. Moreover, the CSR R02 and GFZ R03 + GAB show very similar trend maps (Bettadpur *et al.* 2006). The CSR R02 is not publicly available, so we decided to use the GFZ R03 for mass variation estimates after inclusion of the prescribed corrections.

3 MASS VARIATION ESTIMATES IN ANTARCTICA AND GREENLAND

To calculate the mass variation over the polar regions we must take into account the PGR contribution, which is particularly large in Antarctica. It has already been shown, by means of previous SLR and GRACE analyses (Tosi *et al.* 2005; Chen *et al.* 2006a,b; Lutchke *et al.* 2006; Velicogna & Wahr 2005, 2006a,b), that PGR trades off with present-day mass imbalance in Antarctica and Greenland. This ultimately means that mantle viscosity, controlling the present-day mass variation due to PGR, impacts mass variation estimates due to present-day ice mass imbalance, the latter depending only on the elastic properties of the Earth.

In our analysis, mass variations seen by GRACE and the PGR contribution are considered separately. In order to accurately isolate the PGR signal in the GRACE time-series, we perform a thorough search in the PGR model parameter space. GRACE-derived and PGR computed mass variations are of different nature: PGR mass changes are derived from a model, which means that they can be computed at any prescribed spatial resolution. The PGR signal will be computed at the same spatial resolution used in our treatment of GRACE data, meaning that in both cases we truncate at the same harmonics degree 70. The spatial resolution of experimental GRACE observations is instead limited by noise and various sources of error, and our analysis is aimed at recovering a realistic estimate (not necessarily precise) of mass variations to be compared with the PGR results. Thus, mass variations from GRACE time-series and PGR will be combined to estimate present-day ice mass imbalance in Antartica and Greenland only in the final stage of our work.

3.1 Treating the noise

The short wavelength components of the gravity field are affected by noise, which limits the spatial resolution of the derivable information. For this reason, GRACE data have to be processed in order to reveal geophysical signals. Typically, some sort of smoothing is necessary to remove random noise and make the *true* signal emerge: by substituting the unprocessed signal with a suitable local average at any point in space, the spatial resolution decreases. Moreover, when a smoothing filter is applied to the points near the boundaries of the selected areas, signal belonging to the outer part is mixed to the internal signal producing *leakage*.

The most commonly employed filter is the Gaussian smoothing: it acts as a low pass filter, and it is characterized by half-width at half-maximum in km. The spectral representation of the Gaussian filter (W_ℓ) is available and thus it is easy to obtain a filtered $\Delta\sigma$ by multiplying GRACE harmonic coefficient by W_ℓ in eq. (2). Wahr *et al.* (1998) introduced this averaging method based on a simple Gaussian filter applied to GRACE data.

However, smoothing alone is not sufficient in presence of correlated noise, since in this case a moving average filter over relatively small areas does not average to zero, even in principle. Unfortunately, GRACE data exhibit this kind of noise, and it appears in the unprocessed GRACE maps in form of long linear features in the north–south direction, commonly known as stripes (Swenson & Wahr 2006). The source of these errors is not clear, so they cannot be removed *exactly*. However, specific filters have been proposed and applied (Chambers 2006; Swenson & Wahr 2006). Much care must be used, though, as they also affect the true physical signal to an extent and with a spatial pattern that is not trivial to estimate.

In our work, we choose our own processing strategy for GRACE data. Differently from other recent works on the subject, we choose

to adopt a processing as simple as possible, and we perform the necessary smoothing applying simple Gaussian filters. We also perform the same calculation using the Chambers mass grids, that are preventively destriped according to Chambers recipe (Chambers 2006). We can thus compare the results obtained using the two different processing of GRACE data, and estimate the effect related to different treatments. Since destriped data require less smoothing and so the leakage effects are smaller, a comparison of results obtained with and without destriping would require different smoothing sizes. Chambers mass grids are given with a smoothing expressed as the half-width of the equivalent Gaussian smoother: 400, 500 and 750 km.

3.2 Averaging function

The very basic way to obtain the total mass variation from a specific region is to integrate the mass distribution $\Delta\sigma_t$ over the *Region* as in eq. (1), or integrating over a sphere the $\Delta\sigma_t$ multiplied by a *Region* function $R(\theta, \phi)$ defined as follows:

$$R(\theta, \phi) = \begin{cases} 0 & \text{outside } Region \\ 1 & \text{inside } Region. \end{cases} \tag{3}$$

This is also called exact averaging kernel, and we applied it to the Chambers mass grids to obtain the monthly values of Fig. 1.

The first step to smooth the observational and truncation errors is to use a smooth averaging kernel obtained by convolving the *Region* function $R(\theta, \phi)$ with a Gaussian filter. The results obtained with a smooth averaging kernel are equivalent, on the other hand, to an integration of $\Delta\sigma_t$ smoothed with a Gaussian filter.

Swenson & Wahr (2002) developed a technique to extract regional mass anomalies from GRACE gravity coefficients by means of refined averaging functions. This technique aims at isolating the gravity signal of an individual region while simultaneously minimizing the effects of GRACE observational errors and contamination from the surrounding glacial, hydrological and oceanic gravity signals.

In the case of pre-treated mass grids like the Chambers ones, it is not possible to apply a refined averaging function and, thus, we can only integrate over the region $R(\theta, \phi)$. In order to obtain results from GRACE data comparable with those obtained integrating Chambers mass grids, we decided not to use refined averaging functions.

The theoretical resolution of GRACE is a few hundred kilometres (less then 500 km) with an accuracy of 2 mm of water equivalent (Wahr *et al.* 1998). For the first years of GRACE data, on the other hand, Wahr *et al.* (2004) have shown that, for the hydrological cycle, filters ranging between 750 and 1000 km result into an accuracy of 1.5 cm. Chen *et al.* (2005) showed that the filters can be reduced from 800 to 600 km when GRACE coefficients are fitted with sine and cosine functions. Tamisiea *et al.* (2005), for Alaska, made a comparison between the mass balance obtained with different filters sizes of 250, 500, 750 and 1000 km, obtaining smaller trends for larger filter sizes and choosing, as the optimal, a width of 500 km.

We tested three different filter sizes, namely 750, 500 and 250 km. We choose to adopt 500 km as the optimal size, in agreement with Tamisiea *et al.* (2005). The difference in the results using different filter sizes provides an estimate of the sensitivity to the filter.

The limited spatial resolution makes the description of localized phenomena difficult, and when smoothing is applied, leakage may become substantial. In particular, the amplitude of the signal in the inner region decreases, while it spreads outside its true boundaries, and signal from the outside areas enters in the inner regions. Sophisticated techniques have been proposed to recover the true signal from that derived from smoothed data, mainly in the form of suitable scaling factors, but the accuracy of these corrections depend on the shape of the geographical regions, and on the spatial pattern of the physical signal, the latter not being known *a priori*. Thus, to avoid misleading assumptions that could introduce artefacts, we privilege a simpler approach.

To provide a rough estimate of truncation and leakage errors at the edges of the regions under study, we performed the calculations over two regions, one reduced and the other expanded by a stripe with respect to the real edges of Antarctica and Greenland: in the following we call them Inner and Outer Regions. The width of the stripe between the Inner and Outer Regions is of one element of the grid, whose resolution corresponds to a truncation of harmonic degree $\ell = 64$. Such a width accounts entirely for Gibbs phenomenon at the edge of the regions of interest, since we truncate at harmonic degree $\ell = 70$ and, partially, for leakage, depending on the smoothing filter.

We thus provide our mass variation estimates not as a single accurate best value, but rather in terms of a variation interval, whose amplitude is estimated through the comparison between the Inner and Outer region integrals: we expect that a realistic physical signal falls inside this variability range. This signal can be directly compared with the PGR calculated signal, that instead is not affected by uncertainties due to noise, but only to our incomplete knowledge of Earth's viscosity and ice history.

3.3 Computation

In estimating the mass variations seen by GRACE, we follow two different but equivalent techniques to extract the linear trends from the time-series.

In the first mode, we calculate the mass variation over the region of interest, Antarctica and Greenland, by integrating the function $\Delta\sigma_t$ (eq. 2) over the region of interest month by month (eq. 1) and then by performing a linear regression on the series of monthly values, obtaining the total mass variation trend $\delta\dot{\sigma}$. This procedure is similar to what Velicogna & Wahr (2005, 2006a,b) did for Antarctica and Greenland. Note that these authors perform the integration using a rather sophisticated averaging function to take care of the leakage and other scaling factors.

In the second mode, we first perform a linear regression on the time-series for each harmonic coefficient $\dot{C}_{\ell m}$ and $\dot{S}_{\ell m}$, and then we calculate the map of the linear trends, finally integrating over the region of interest to obtain the total mass variation trend $\delta\dot{\sigma}$:

$$\delta\dot{\sigma} = \int_{\text{Region}} \Delta\dot{\sigma}(\theta, \varphi) \mathrm{d}\Omega, \tag{4}$$

$$\Delta\dot{\sigma}(\theta, \varphi) = \frac{a\rho_E}{3} \sum_{\ell,m} \frac{2\ell + 1}{k_\ell + 1} \overline{P}_{\ell m}(\cos\theta) \times (\dot{C}_{\ell m} \cos\varphi + \dot{S}_{\ell m} \sin\varphi). \tag{5}$$

This second method offers several advantages in treating the temporal series of the signal, for example by allowing one to remove the periodic (annual–semi-annual) signals separately for each wavelength or harmonic degree. In this work, we perform linear regressions including or removing the annual signal. The two methods are expected to produce similar results in terms of mass variation estimates. Indeed, this double cross-check has been very useful in the debugging stage.

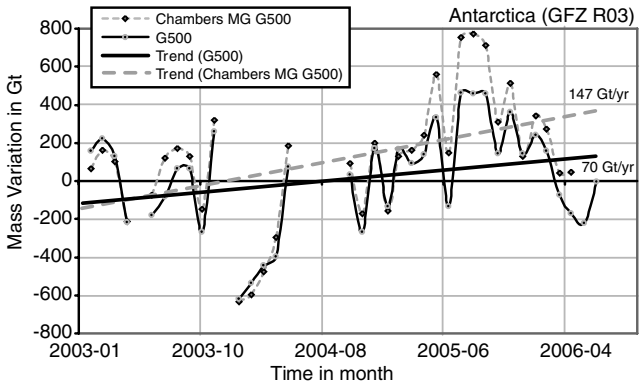

Figure 2. Monthly mass variation in Gt over Antarctica using GFZ R03 GRACE data. The solid black curve with grey squares are obtained within our own analysis using the 500 km Gaussian filter (G500). The width of the Gaussian filter is 500 km. The grey dashed with black diamonds is obtained by integrating, month by month, Chambers mass grids (Chambers MG G500) treated with an equivalent 500 km Gaussian filter. The thick solid black and thick dashed grey lines are the corresponding linear trends.

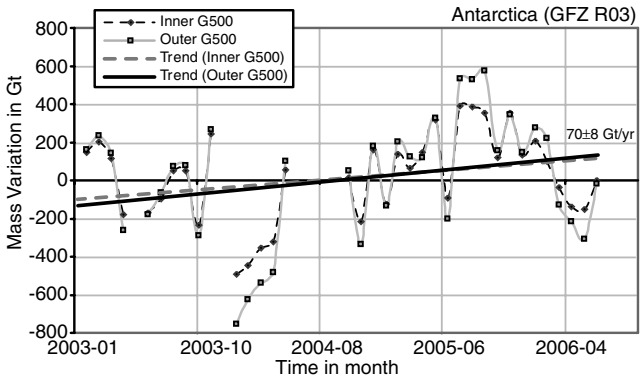

Figure 3. Monthly mass variations over the Outer and Inner Regions for Antarctica, based on GFZ R03. Black thin dashed curve with grey diamonds represents the monthly mass grids for the Inner region, the grey thin solid curve with black squares is obtained for Outer Region. The dashed and solid linear trends refer to the Inner and Outer Regions, respectively. The width of the Gaussian filter is 500 km, as in Fig. 2.

We begin by showing the results obtained from the first method for Antarctica. A first rough but meaningful estimate is obtained by integrating each GRACE monthly solution over the entire Antarctica. This is done by means of a Gaussian filter of 500 km, solid black line in Fig. 2, and can be compared with the time-series obtained with Chambers mass grids with the same equivalent Gaussian width, dashed grey line. As in Fig. 1, note the absence of the four months (from 2004 July to 2004 October). The shape of the function is clearly similar but, as expected, differences appear, probably due to the ocean pole tide correction (or more unlikely the destriping) which is present in Chambers mass grids and not in our calculations. These differences, most evident in the time intervals 2005 June and 2006 April, increase the linear trend from 70 Gt yr^{-1}, that is our estimate, to 147 Gt yr^{-1}, obtained from Chambers mass grids. Although the results obtained from the two data analyses are rather different for Antarctica mass variation estimates, we have no reason to reject one in favour of the other so we keep both the estimates as upper and lower bounds.

We estimate the leakage and the error made at the edge of Antarctica, by computing the integral over the Inner and Outer Regions, as explained above. The linear trends from these calculations can be considered as upper and lower bounds for the errors due to leakage or edge effects along the border of Antarctica; thus we obtain a range of variability that roughly account for the attenuation of the signal caused by filter. In particular, we take into account the maximum of the difference between the two bounds and the trend previously computed over the 'standard' region. We also made tests with different filter sizes, with Antarctica mass variation estimates showing consistency for filter size variations. For example from 500 to 250 km filter size, the estimate 70 Gt yr^{-1} becomes 73 Gt yr^{-1} (gaining less than 5 per cent): this means that the mass variation in Antarctica is poorly affected by the filter size, and the possible loss of signal is around 5 per cent.

Fig. 3 shows the linear trends for the Inner and Outer Antarctica regions, dashed grey and solid black lines, within our own scheme, providing a range of variability of ± 8 Gt yr^{-1}. This estimate is the maximum difference between the trend (70 Gt yr^{-1}) and the trend obtained from Inner and Outer Region. Black and grey squares provide the monthly mass variations for the Inner and Outer Regions, respectively.

Following the same approach with the same filter size of 500 km as in Fig. 2, but for the old CSR release 01 data, Fig. 4 shows different linear trends with respect to Fig. 2, lower with respect to the GFZ release 03 by 23 per cent for the series obtained from Chambers mass grids and by 24 per cent for our direct analysis of GRACE data. These results can explain some discrepancies with respect to previous work on Antarctica based on the old CSR release 01 (Velicogna & Wahr 2006a).

For Greenland, by applying the first method, things are a bit more complicated, because Greenland is smaller than Antarctica and, as we will see, mass variations are concentrated at the edge, where errors due to leakage, edge effects and noise are expected to be large. In fact, most of the GRACE noise is concentrated at high harmonic degrees which means that small spatial details (like mass variations on the Greenland edges) can be easily overestimated. For these reasons, we obtain that for Greenland the variability among the results obtained using different filters and when dealing with the Inner and Outer Regions is larger than for Antarctica. Fig. 5, analogous to Fig. 2 with the same 500 km filter, shows that -67 Gt yr^{-1} is obtained within our own direct analysis, to be compared with -45 Gt yr^{-1} obtained from the Chambers mass grids (GFZ R03).

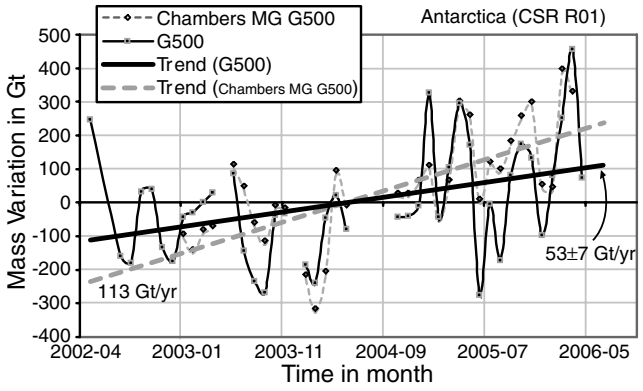

Figure 4. Same as in Fig. 2, for the old CSR R01, for Antarctica. The solid line is obtained using our scheme, and includes the bounds obtained with the Inner and Outer regions.

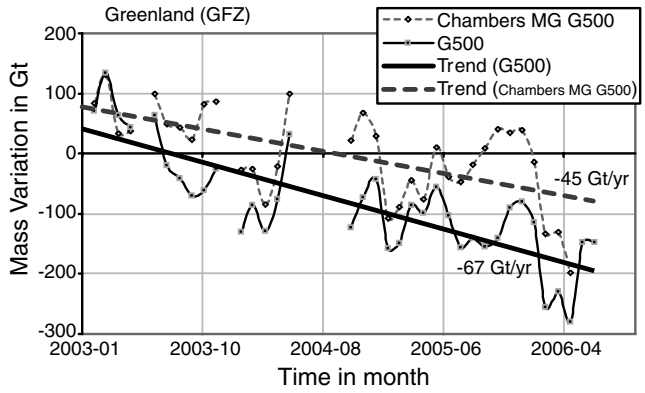

Figure 5. Same as in Fig. 2, for Greenland.

Table 1. Mass trends in Antarctica and Greenland computed from GRACE.

	Antarctica (Gt yr^{-1})	Greenland (Gt yr^{-1})
Using GFZ R03 (G250)	73 ± 10	-88 ± 36
Using GFZ R03 (G500)	70 ± 8	-67 ± 22
Using Chambers MG GFZ	147	-45

We have verified that, in contrast to estimates for Antarctica, the use of different filters impacts mass variation estimates. Reducing the filter down to 250 km, we obtain, within our own scheme, -88 Gt yr^{-1} instead of -67 Gt yr^{-1} of Fig. 5, which can be taken as the lower bound, since a further reduction in the size of the filter would certainly overestimate the error. By applying the same procedure in the Inner and Outer Regions, we obtain a range of variability in terms of upper and lower bounds, -67 ± 22 and -88 ± 36 Gt yr^{-1}, respectively. The range of variability for Greenland is about a factor three or four larger than for Antarctica, since the largest mass changes in Greenland occur in proximity of its edge. This means that the surface where mass changes are concentrated is smaller than the entire Greenland continental area, which is, in turn, smaller than Antarctica, where ice masses are widespread.

Table 1 summarizes the estimated mass variation trends from GRACE data in Antarctica and Greenland. It is notable that the trend of -45 Gt yr^{-1} obtained from Chambers mass grids in Fig. 5 coincides with the lower bound of our estimate, once the range of variability of 22 Gt yr^{-1} is considered with our estimate of -67 Gt yr^{-1}. In contrast to the Antarctica case, the same analysis on CSR R01 data gives slightly different trends from the ones obtained with GFZ R03 and within the range of variability even though the time-series are rather different. For these reasons, the results obtained from CSR R01 for Greenland will not be considered further.

By applying the second method based on the linear regression of single gravity coefficients as described above, we obtain the map of the mass variation trend in Fig. 6(a), once the linear trends of each harmonic coefficients are summed together; a Gaussian filter of 500 km has been used, in agreement with the previous analysis. Major features are the red spots of mass growing over Hudson bay and Gulf of Bothnia, clearly due to the PGR induced uplift of the crust, the mass decrease in Greenland, at its southeastern edge, and the blue and red spots of decreasing and increasing mass in Antarctica, close to each other, at 240 and 290 longitude degree. Other features can be generally interpreted in terms of hydrological effects. This second method of treating GRACE data provides the same results as the first one described above, once our scheme is

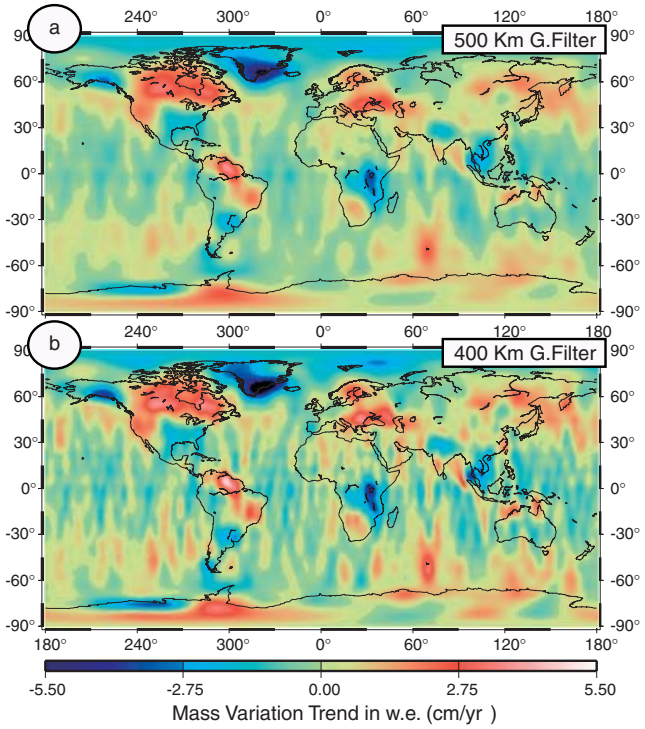

Figure 6. Map of mass variation trend in water equivalent (w.e.), expressed in cm yr^{-1}. The trend map, based on the linear regression of individual gravity coefficients, is smoothed with a 500 km Gaussian filter, panel a, and with a 400 km one, panel b.

considered. The coincidence provides the evidence that our procedures are consistent.

The lower filter of 400 km makes some details more evident in Fig. 6(b), though disturbed by the presence of longitudinal stripes. The Fig. 7, where the 250 km filter has been used, makes it more evident that most of the mass loss is concentrated at the southern edge of Greenland (Fig. 7a), once compared with Figs 6(a) and (b). With the 250 km filter for Antarctica (Fig. 7b), the noise (stripes) makes the interpretation rather difficult.

We also computed separately in the same way the contributions from the Western and the Eastern parts of Antarctica. Without considering the PGR contribution, the mass variations in Western and Eastern Antarctica, for our own data analysis are 43 and 26 Gt yr^{-1}, respectively, while for those obtained from Chambers mass grids are 123 and 24 Gt yr^{-1} (first two rows in Table 5).

4 THE PGR CONTRIBUTION

As anticipated, we want to take into account the PGR signal, conveniently converted into water equivalent units. We calculated the rate of geoid variation, in millimetre per year, due to PGR on the basis of the ICE-3G ice-sheet model for the Pleistocene (Tushingham & Peltier 1991), and for an earth model characterized by viscosities of 10^{20} Pa s in the upper mantle and 10^{22} Pa s in the lower mantle. Deglaciation centres produce spots of geoid increase over Hudson bay and Antarctica that can be as large as 2 mm yr^{-1}, due to the uplift of the Earth's crust, where crustal material substitute the air or the water, of lower density.

The PGR induced geoid is characterized by a smooth pattern. The time dependent surface density anomalies due to PGR can be con-

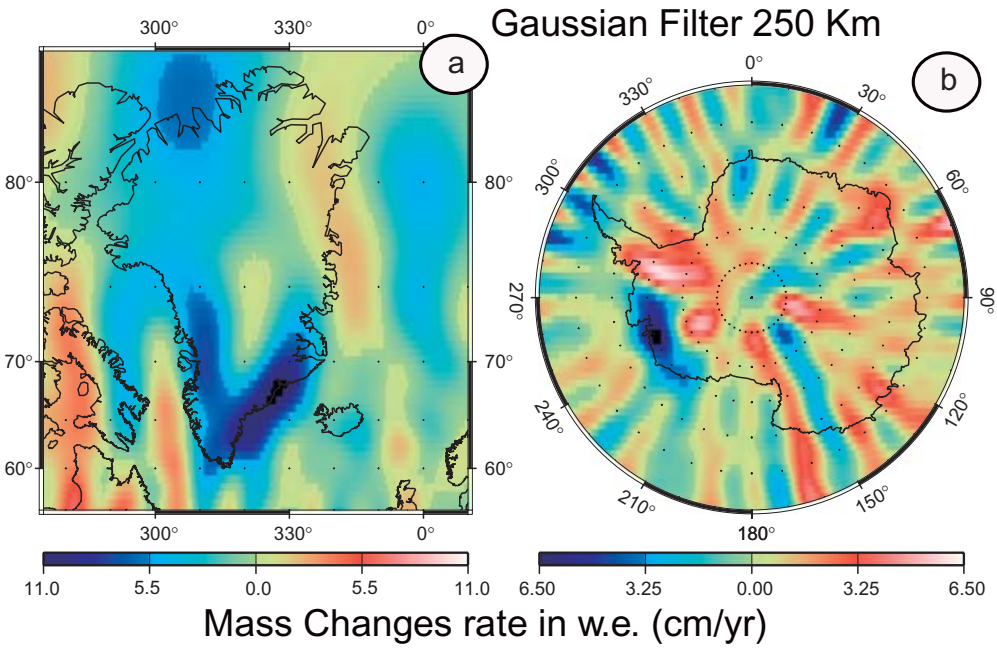

Figure 7. Rate of mass changes in water equivalent (cm yr^{-1}) over Greenland, left-hand panel, and Antarctica, right-hand panel, for a Gaussian filter of 250 km.

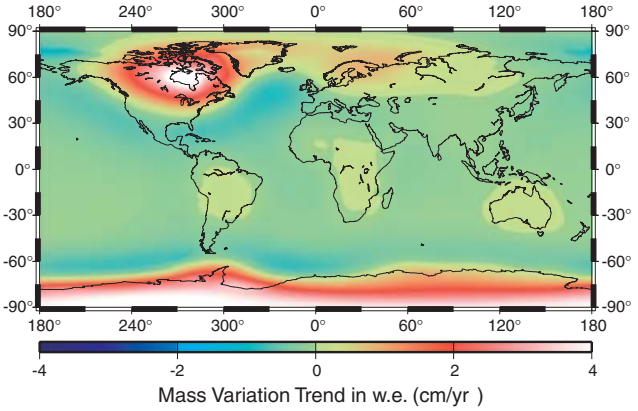

Figure 8. PGR mass variation trend in water equivalent (cm yr^{-1}). The earth model is given in Table 2.

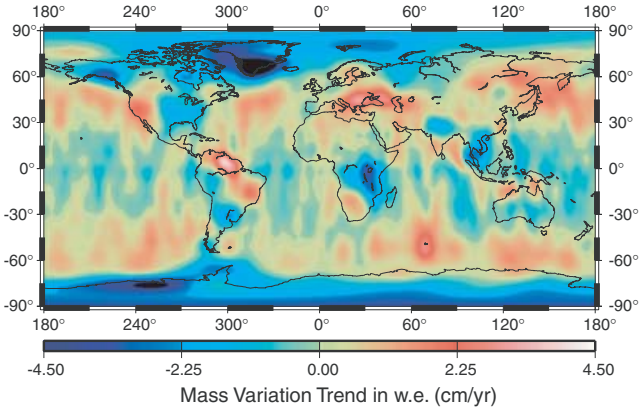

Figure 9. GRACE mass variation trend in water equivalent, after removal of PGR contribution, based on the model parameters of Table 2.

verted into water equivalent units, as in Fig. 8. Over the deglaciation centres, we have an increase in water equivalent ranging between 4 cm yr^{-1}, over Hudson Bay and Antarctica, or about 2 cm yr^{-1}, over the Gulf of Bothnia, while over the peripheral oceanic and continental areas we note a decrease of 0.5 to 1.0 cm yr^{-1}, due to the downflexure of the portion of the lithosphere in the periphery with respect to the uplifting deglaciation centres. It is also notable that over continental areas, such as central Africa, south America and Australia, we obtain a slight water equivalent increase, of about 2–3 mm yr^{-1}, due to a slight uplift of the continents caused by the levering effects of the subsiding oceanic basins, as described in Mitrovica & Peltier (1991).

Fig. 9 shows a qualitative map of the mass variation trend, obtained by subtracting the PGR contribution from GRACE trends, which means subtracting PGR trends of Fig. 8 from Fig. 6(a). The PGR trends map is truncated at 70 harmonic degree in order to match the spatial resolution of the GRACE trends map; since the GRACE data are filtered a straight subtraction with unfiltered PGR trends is not completely correct. We should filter the PGR, loosing signal, or, in order to recover the lost signal in GRACE trends map, we should perform some sophisticate processing, for example deriving a spatial dependent scaling factor or designing a refined filter to reduce leakage effects, that could make the whole analysis less transparent. So Fig. 9 is meant to be only a qualitative map to show the typical pattern of mass variation trend.

Once compared with Fig. 6(a), it is notable that the large spot over Hudson Bay disappears, making this region actually quite stable, and the gravity gain over Scandinavia is also reduced. In Antarctica, the increase in water equivalent seen in GRACE data at 290° longitude is disrupted by subtraction of PGR effects and the decrease observed in Fig. 6(a) in the spot of Western Antarctica at 240° is enhanced.

4.1 Varying the earth model

Figs 8 and 9 are based on a single PGR model, in terms of both unloading history and Earth's viscosities. We now quantify PGR signal

Table 2. Reference rheological structure of the employed five layered Earth.

Layer	Radius (km)	ρ (kg m^{-3})	μ (Pa)	ν (Pa s)
1	6371.0	3196.9	5.98×10^{10}	1.00×10^{50}
2	6250.0	3457.7	7.41×10^{10}	1.00×10^{20}
3	5951.0	3882.3	1.09×10^{11}	1.00×10^{20}
4	5701.0	4890.6	2.21×10^{11}	1.00×10^{22}
5	3480.0	10925.	0.00	0.0

variations once different earth models and deglaciation histories are employed, showing at the same time how PGR modelling impacts our interpretation of GRACE results.

By means of normal mode relaxation theory for an incompressible, viscoelastic, stratified Earth, based on analytical fundamental matrix (Sabadini *et al.* 1982), we make use of the five layers earth model described in Table 2 in terms of major rheological and viscosity layering, volume averaged according to the PREM model (Dziewonski & Anderson 1981). We change the thickness of the lithosphere from 80 to 200 km, and the viscosity of the upper and lower mantle, with respect to the reference model of Table 2. As we will show, the viscosity has the major impact on the final results. Recent works on inversion with PGR and present-day deglaciation predictions (Tosi *et al.* 2005), favour an upper-mantle viscosity of 10^{20} Pa s and a lower mantle viscosity of 10^{22} Pa s. To calculate the effects of the deglaciation, we take into account also the effects due to sea level variations. We change the model performing two tests with and without the sea level contribution, respectively, and a third test, for ice-sheet melting limited to Antarctica, neglecting the ICE-3G deglaciation contributions occurring outside Antarctica. The PGR contribution, in contrast to Chen *et al.* (2006a), has not been filtered but, as anticipated, we take into account the harmonics up to degree 70 (as we did with GRACE data) and so we consider all the information contained in the modelling, the latter being exact in nature, with uncertainties depending only on our incomplete knowledge of Earth's viscosity and ice history.

We calculate for each PGR model, the mass variation trend $\Delta\dot{\sigma}(\theta, \varphi)$ (eq. 5), and then for each region (Antarctica and Greenland) we integrate over the region to obtain $\delta\dot{\sigma}$, the total mass variation trend for that region. In order to estimate the weight of the variation in the PGR model, we made three tests.

In the first we fixed the lithospheric thickness and upper–lower-mantle viscosity and we calculated the $\delta\dot{\sigma}$ using the three different deglaciation processes depicted above, or different loadings, namely ICE-3G including the effects of sea level equation, ICE-3G without solving for the sea level equation and considering melting from ICE-3G limited to Antarctica.

Then we calculate the mean deviation, in Gt yr^{-1}, between the three values (two in case of Greenland):

$$\text{Mean Dev} = \frac{1}{N}\sum_{i=1}^{N} |x_i - \overline{x}|, \tag{6}$$

where N is the number of values (3 or 2), x_i are the values, and $\overline{x}$ is the average of the N values.

Fig. 10 shows for each lithospheric thickness and for each upper–lower-mantle viscosity combination, the mean deviation between the results given by the different deglaciation processes. The mean deviation, in Gt yr^{-1}, represents the variability range in the final results by using one unloading history instead of another. For Antarctica the mean deviations are lower than 20 Gt yr^{-1}, for all viscosity combinations, and for Greenland, they are lower than 4 Gt yr^{-1}. The average of the ratio between the mean deviation and the mean values are the percentage above the triplets, and they represent the PGR sensitivity to the unloading history.

In the case of the most appropriate mantle viscosity combination (Tosi *et al.* 2005), 10^{20}–10^{22} Pa s and 10^{21}–10^{22} Pa s, the PGR sensitivity is small. This means that present-day mass variation in Antarctica and Greenland is rather insensitive to details of ice loading in north America and northern Europe, and on the way in which the water is redistributed in the oceans.

In the second test we fixed the deglaciation process and upper–lower-mantle viscosity, we calculated $\delta\dot{\sigma}$ using the three different lithospheric thicknesses, and then we calculated the mean deviation, in Gt yr^{-1}, between the three values with the eq. (6). Similarly to Fig. 10, for each of the three loads introduced above and for each upper–lower-mantle viscosity combination, Fig. 11 shows the mean deviation between the different lithospheric thicknesses, namely 80, 121 and 200 km. For Antarctica the mean deviations are lower than 20 Gt yr^{-1}, for almost all viscosity combinations, and for Greenland, they are lower than 6 Gt yr^{-1}. As in Fig. 10, in the case of the most appropriate mantle viscosity combination the PGR sensitivity is small for Antarctica. For Greenland there is a substantial increase in the sensitivity to lithospheric thicknesses variations.

The most notable effects in PGR modelling become visible when we vary the mantle viscosity, as in Fig. 12. Here we use the average over the results computed with the three lithospheric thicknesses, and the three unloading histories (two for Greenland).

For each upper- and lower-mantle viscosity we obtain the mass variation values in giga-tons per year over Antarctica and Greenland by integrating mass changes over these continents, as shown in the graphs. The grey bars stand for the mean deviation (with respect to the average), as in eq. (6). The positive mass variations, due to uplift of the crust, are extremely sensitive to mantle rheology. Over the area of Antarctica, mass trends varies from about 20 Gt yr^{-1}, for 10^{19}–10^{20} Pa s, to about 279 Gt yr^{-1}, for 10^{21}–10^{22} Pa s. A stiffer lower mantle relaxes slowly, so at present it is still strongly rebounding, while a soft lower mantle has already relaxed almost completely, so the present-day gain in crustal material replacing air or water is small. It is notable that for the most realistic lower mantle viscosities of 10^{21}–10^{22} Pa s, the PGR signal for Antarctica remains rather constant for upper-mantle viscosity ranging in the 10^{20}–10^{21} Pa s interval.

In contrast, Greenland's signal is sensitive to upper-mantle viscosity, with a drastic reduction in PGR contribution for 10^{20} Pa s with respect to 10^{21} Pa s. For both cases of Antarctica and Greenland, the extremely low and unlikely 10^{19} Pa s upper-mantle viscosity dampens completely the PGR contribution, since the upper mantle is completely decoupled from the lower mantle and the whole relaxation occurs in the upper mantle. The upper–lower-mantle viscosity combination 10^{19}–10^{21} Pa s is too low and unlikely, so we do not consider it in estimating the PGR lower bound contribution; 10^{20} Pa s and 10^{21} Pa s are low but acceptable so we can use the corresponding mass variation as a lower bound.

From Fig. 12 we thus extract the lower and upper bounds for PGR contributions in Antarctica and Greenland, reported also in Table 3. For the upper bound of PGR contribution in Antarctica, we take the maximum of the values corresponding to the upper-mantle viscosities of 10^{21} Pa s, namely 279 ± 18 Gt yr^{-1} (grey bars in Fig. 12). Excluding the upper–lower-mantle viscosity 10^{19}–10^{21} Pa s, for the reason explained above, the lower bound for the PGR contribution in Antarctica is the minimum of the values, which gives 59 ± 3 Gt yr^{-1}. In a similar way, for Greenland, we obtain an upper bound PGR contribution of 34 ± 6 Gt yr^{-1}. For the lower

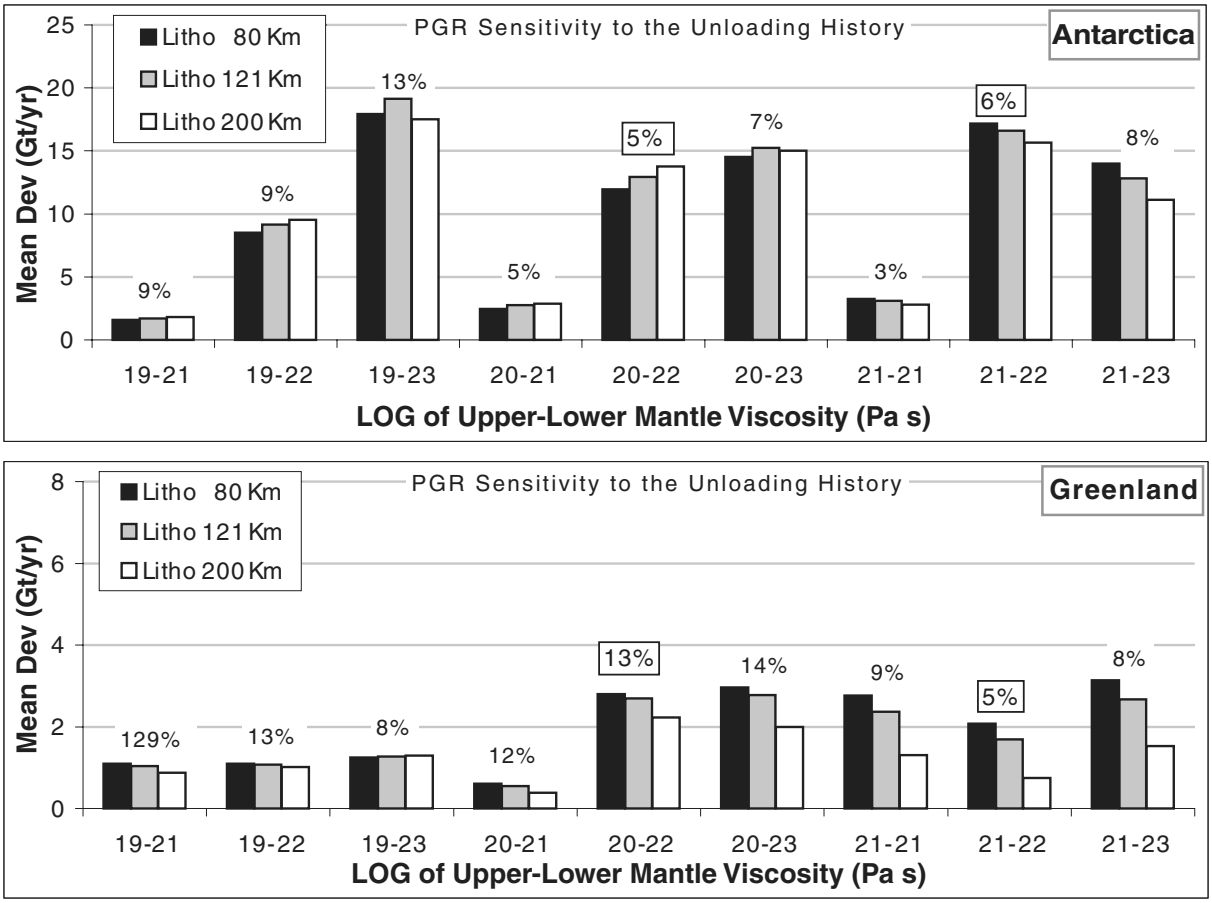

Figure 10. This figure shows, for different viscosity combinations, as given in the bottom scale, and for three lithospheric thicknesses, as given in the legends, the mean deviation among the results obtained using the various deglaciation processes.

bound we used the 5 ± 1 Gt yr^{-1} (rounded up) corresponding to upper-mantle viscosities of 10^{20} Pa s.

Our lower and upper bounds for PGR contribution in Antarctica can be compared with the corresponding estimate by Velicogna & Wahr (2006a) providing 113 Gt yr^{-1} as lower bound and 271 Gt yr^{-1} as upper bound. Although based on a similar analysis, Velicogna & Wahr (2006a) used different PGR models with respect to ours. Our PGR range 59–279 Gt yr^{-1} is evidently wider because we considered also extreme viscosity values, as shown above, but the resulting average values of 192 ± 79 Gt yr^{-1} by Velicogna & Wahr (2006a) and our value of 169 ± 110 Gt yr^{-1} are rather in agreement, demonstrating the validity and robustness of PGR modelling, in terms of both loading history and Earth viscosity models.

The PGR contribution must be subtracted from GRACE mass variations in order to estimate the present-day mass balance in Antarctica and Greenland. Table 4 reports our final results obtained combining our own (upper–lower bounds) mass variation estimates from GRACE data with the upper and lower bounds from PGR contribution. For Antarctica, subtracting from our estimate of 70 Gt yr^{-1}, representing a lower bound in terms of the various GRACE analyses, the lower bound of Antarctica PGR of 59 Gt yr^{-1}, we obtain the lower bound for present-day ice loss in Antarctica of 11 Gt yr^{-1}. Since the given error bounds, for GRACE analysis and for PGR modelling, are not real errors (standard deviation) but represent a range of variability, even if they are independent quantities, we decided to simply sum the two range in order to obtain the final estimate. So the range of variability of ± 11 Gt yr^{-1}, is the sum of the two range of variability ± 8 Gt yr^{-1}, for the Inner and Outer Regions, with ± 3 Gt yr^{-1}, from PGR modelling. The lower bound for present-day mass balance (largest ice loss) in Antarctica is obtained by subtracting 279 Gt yr^{-1}, the PGR upper bound, from our own estimate of GRACE mass recovery over Antarctica of 70 Gt yr^{-1}, providing -209 Gt yr^{-1}. These values are summarized in the first row of Table 4.

The upper bound, instead, is obtained by subtracting from the mass variation estimate from GFZ Tellus, 147 Gt yr^{-1}, the PGR lower bound of 59 Gt yr^{-1}, providing an accumulation of $+88$ Gt yr^{-1}. Subtracting the PGR upper bound of 279 Gt yr^{-1}, we obtain -132 Gt yr^{-1} of ice loss. These values are summarized in the second row of Table 4. The third and fourth rows of Table 4 present the results of the same analysis applied to the CSR solution, resulting into a generally higher ice loss in Antarctica, including a reduced accumulation of $+54$ Gt yr^{-1}, instead of $+88$ Gt yr^{-1} of the GFZ 03 release, when the PGR lower bound is considered.

Performing the same analysis for Greenland provides an upper bound for present-day melting of -122 Gt yr^{-1} by subtracting from our own estimate of linear mass variation of -88 Gt yr^{-1} the PGR upper bound for Greenland of 34 G yr^{-1}, provided in Table 3. Accordingly, the lower bound -45 Gt yr^{-1} obtained from Chambers mass grids GFZ, Fig. 5, minus the PGR lower bound of 5 Gt yr^{-1}, resulting into -50 Gt yr^{-1} (rounded up) of present-day ice mass loss over Greenland. The other bounds for the various GRACE data analyses given in Table 4 can be obtained by subtracting the lower and upper bounds of PGR contribution from the

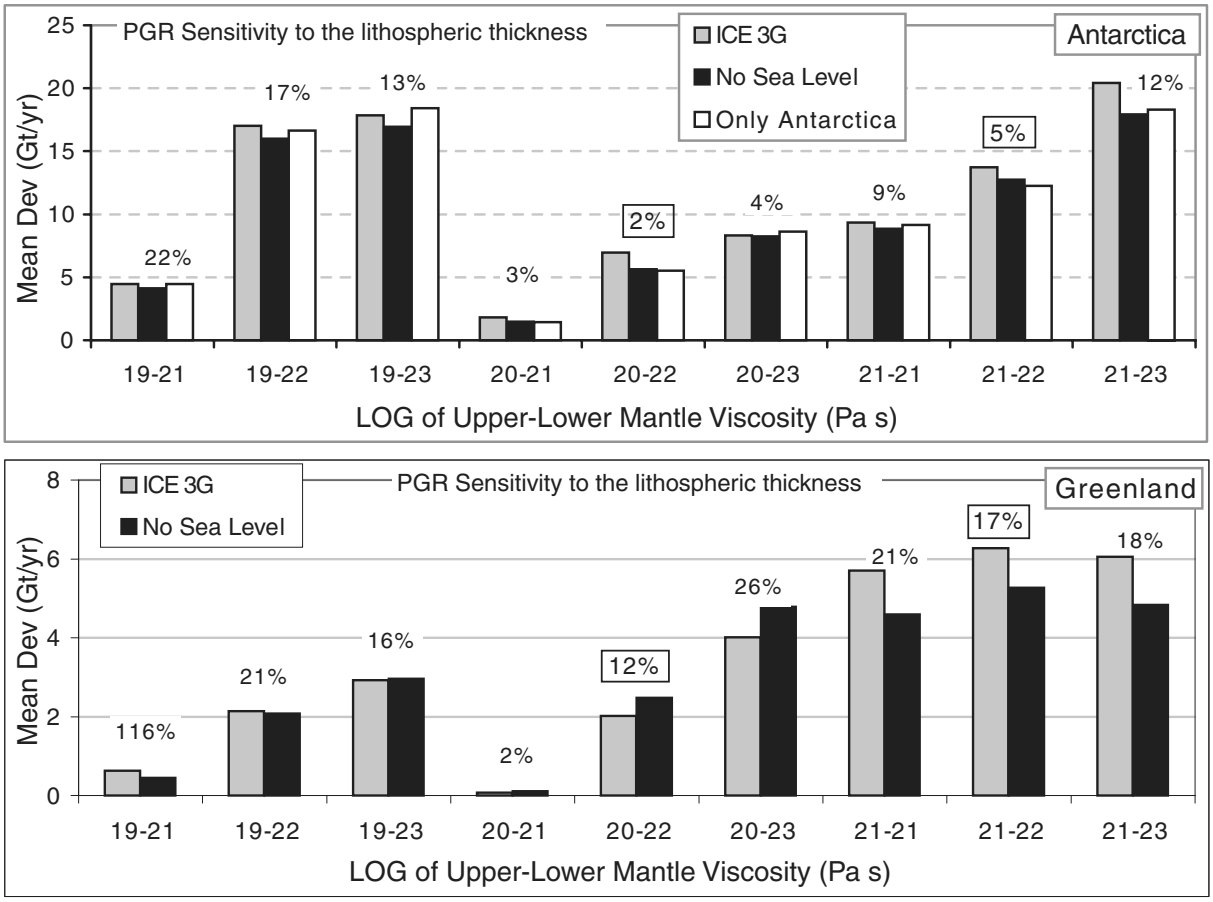

Figure 11. This figure shows, for different viscosity combinations, as given in the bottom scale, and for different deglaciation processes, as given in the legends, the mean deviation among the results obtained using the three lithospheric thicknesses.

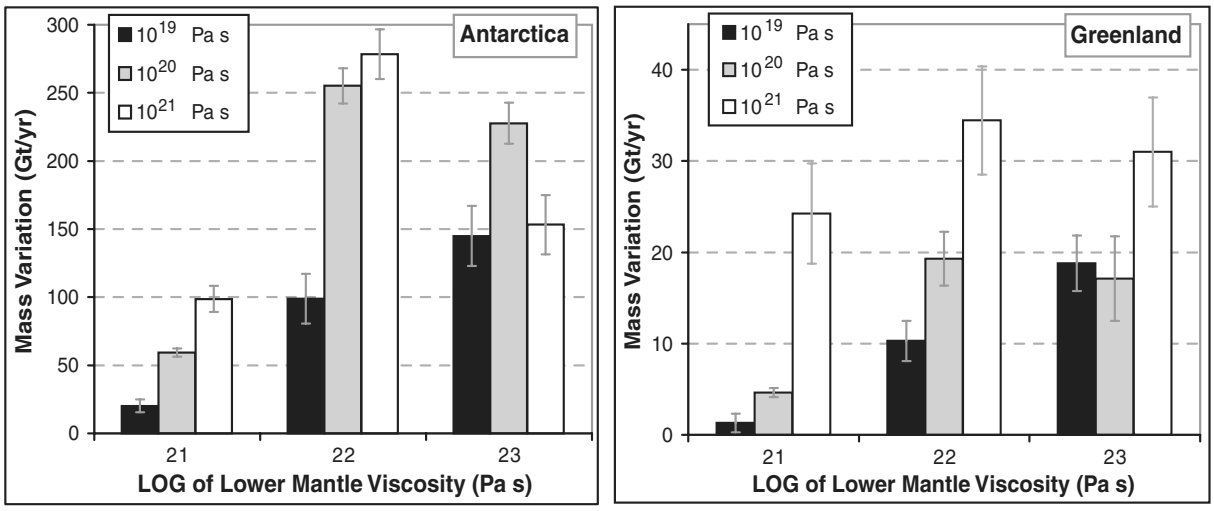

Figure 12. Mass variation in Gt yr^{-1} as a function of lower mantle viscosity for each upper-mantle viscosity, as given in the legends. The mass variation is the average value obtained by using all lithospheric thicknesses and all the deglaciation processes. Vertical grey bars denote the mean deviation from the average.

appropriate estimates of Greenland ice loss based on the different solutions.

Table 4 thus provides the complete bounds by considering all GRACE data analyses and their possible combination with PGR bounds. The large variability in the results is clear, resulting mostly from the earth model chosen for the PGR simulation, but also the treatment of the GRACE data plays a significant role. The Max PGR values give an important ice mass loss both in Antarctica and Greenland, while the Min PGR values give a gain of mass in Antarctica and a limited mass loss in Greenland.

Table 3. PGR final results. Upper and lower bounds for the PGR contribution to mass trends in Antarctica and Greenland.

	Lower bound (Gt yr^{-1})	Upper bound (Gt yr^{-1})
Antarctica	59 ± 3	279 ± 18
Greenland	5 ± 1	34 ± 6

Table 4. Cross-results of mass variation trends obtained combining GRACE data and the PGR models.

	PGR Min (Gt yr^{-1})	PGR MAX (Gt yr^{-1})
Antarctica		
Using GRACE GFZ R03	$+11 \pm 11$	-209 ± 26
Using Chambers MG GFZ	$+88 \pm 3$	-132 ± 18
Using GRACE CSR R01	-6 ± 10	-226 ± 25
Using Chambers MG CSR	$+54 \pm 3$	-166 ± 18
Greenland		
Using GRACE GFZ R03	-72 ± 23	-101 ± 28
Using Chambers MG GFZ	-50 ± 1	-79 ± 6
Lower bound estimate GFZ	-93 ± 37	-122 ± 42

Note: MG stands for Mass Grids.

Our findings imply that Greenland is loosing mass, but Antarctica mass variation ranges from ice loss of -209 Gt yr^{-1} to accumulation at a rate of $+88$ Gt yr^{-1}.

It should be pointed out, on the other hand, that not all the PGR models are equally plausible, so that in Table 4 it is certainly possible to make a choice between the column PGR Min and PGR Max, by taking account recent findings on mantle viscosity profile from a variety of geophysical data, such as in Mitrovica & Forte (2004) and Tosi *et al.* (2005). The latter is based on self-consistent inversion based on Levenberg–Marquardt schemes of long wavelength time dependent zonals of the gravity field from SLR data and PGR models of the same family as those considered in the present analysis. From these previous analyses the viscosity of the lower mantle is 10^{22} Pa s, and that of the upper mantle is 5×10^{20} Pa s. From Fig. 12, where the second column corresponds to 10^{22} Pa s, and upper-mantle viscosity ranges between 10^{20} and 10^{21} Pa s, in agreement with the SLR inversion, the preferred PGR model yields the largest signal in Antarctica of 279 Gt yr^{-1}. This preferred model forces us to choose the right column in Table 4 for ice-mass loss in Antarctica that, by averaging between mass variations obtained from GFZ Tellus release 03 and our own analysis, in order to take account for the impact of various data treatment modes, yields -171 ± 39 Gt yr^{-1} (rounded up). The range of variability of ± 39 Gt yr^{-1} is half of the difference between the two extrema, in order to have them included in this best estimate. It is notable that this estimate agrees, within the range of variability, with that obtained by Velicogna & Wahr (2006a) of -152 ± 80 Gt yr^{-1}, where the uncertainty derives from the PGR contribution.

For Greenland in the right column in Table 4 there are three values, so we take the mean of the three value and we obtain for the best estimate -101 ± 22 Gt yr^{-1}. The range of variability of ± 22 Gt yr^{-1} is half of the difference between the two extrema, as above.

Performing the same analysis, using the data of Table 5, for Antarctica we can also give the estimates for the Western and Eastern part separately, reported in Table 6. For East Antartica our estimate agrees with the one obtained using Chambers mass grids, and in both cases it indicates that Eastern Antartica is loosing mass. The Western Antartica mass balance is negative only if we consider the PGR contribution based on the optimal viscosity profile (PGR MAX column), as previously pointed out.

Table 5. Mass trends in Antarctica computed from GRACE data and from PGR models: western and eastern part.

Antarctica	West (Gt yr^{-1})	East (Gt yr^{-1})
Using GFZ R03 (G500)	43	26
Using Chambers MG GFZ	123	24
PGR MAX	165 ± 11	119 ± 8
PGR Min	32 ± 2	18 ± 2

Table 6. Mass variation trends for both eastern and western Antarctica obtained combining GRACE data and the PGR models.

	PGR Min (Gt yr^{-1})	PGR MAX (Gt yr^{-1})
West		
Using GRACE GFZ R03	$+11 \pm 2$	-122 ± 11
Using Chambers MG GFZ	$+91 \pm 2$	-42 ± 11
East		
Using GRACE GFZ R03	-6 ± 2	-95 ± 8
Using Chambers MG GFZ	-8 ± 2	-93 ± 8

Note: MG stands for Mass Grids.

4.2 Comparison with previous analyses

Several recent results from other works, derived from GRACE data and other sources, span a rather wide range both for Antarctica and Greenland. It is on the other hand remarkable that all the estimates concur to support the evidence of ice mass loss in both Antarctica and Greenland, as first proposed in Tosi *et al.* (2005) on the basis of a self-consistent inversion scheme on long wavelength time dependent gravity field of a longer time span, twenty years of data, with respect to GRACE. With respect to SLR Tosi *et al.* (2005) estimate of -240 Gt yr^{-1}, our GRACE based estimate of -171 ± 39 Gt yr^{-1} is about 30 per cent lower, although the difference falls to 10 per cent if the range of variability is considered.

When compared with the Velicogna and Wahr Velicogna & Wahr (2006a) estimate of -152 ± 79 Gt yr^{-1}, our value of -171 ± 39 Gt yr^{-1} is in agreement, even if the data set are different, the methods being comparable.

As far as Greenland is concerned, our preferred ice mass loss of -101 ± 22 Gt yr^{-1} agrees well with SLR retrieved mass imbalance (Tosi *et al.* 2005), with Velicogna & Wahr (2005), Ramillien *et al.* (2006) and Lutchke *et al.* (2006) analyses, while it is much lower, by a factor of about 2, than Velicogna & Wahr (2006b) and Chen *et al.* (2006b). It should be pointed out that from SLR analysis, the relative ice discharges between Antarctica and Greenland is rather well constrained, Antarctica always loosing mass more than Greenland, within a self-consistent inversion scheme, which makes us confident of the findings obtained in the present analysis of GRACE data, with both Antarctica and Greenland loosing ice mass, but with Antarctica melting more than Greenland.

The comparison with the results of other recent works based on GRACE data is particularly interesting, as the values obtained are significantly different from ours, in some cases. Some difference is expected, as we performed a simplified treatment. Nonetheless, we try to understand the reason for the discrepancy. Velicogna & Wahr (2006a,b) and Chen *et al.* (2006a,b) use the CSR 01 data; as we showed previously, they produce rather different results from those of subsequent releases, and so some of the discrepancy can be

ascribed to this fact. Moreover, in both works a sophisticated correction is applied to data in order to keep the leakage effect under control. Chen *et al.* (2006b) obtain a global trend map that is very similar to ours, but they then apply a scaling factor of about 2 to correct the leakage effects. This factor is derived from the comparison of the patterns of mass trend derived by GRACE data and from numerical simulations of the effects of an hypothetical mass change source distribution described with the same resolution of GRACE data. The method is rather involved, and it is not clear which is the accuracy in estimating the scaling factor: a smaller scaling factor would produce results similar to ours. In a different way, Velicogna & Wahr (2006b) adopt a combination of sophisticated averaging function designed to minimize the leakage effect. Due to the particular choice of the functions, they also need to scale the results obtained to recover part of the true signal lost in the procedure. For example, for Greenland the scaling is tuned in order to enhance the description of mass variations near the margins, where melting has accelerated according to independent laser altimeter surveys. This choice, together with the limited spatial resolution of GRACE data, may turn into an underestimation of the signal from inner regions, where the same surveys suggest some mass accumulation: the non-uniform distribution of mass change sources, as indicated for example from altimetric measurements (Zwally *et al.* 2005), can make the use of a single scaling factor a choice whose accuracy is very difficult to assess *a priori*.

Ramillien *et al.* (2006) use geoid solutions from GRACE data, 10-d interval from 2002 July to 2005 March, computed by an independent centre. They find mass loss (-129 ± 15 for Greenland and -169 ± 39 for Antarctica) lower than in the comparable Velicogna & Wahr (2006a,b), and they attribute these differences to the different geoid solutions and to different PGR modelling, but we think that the different treatment of leakage has a role too.

Lutchke *et al.* (2006) compute ice mass variations in Greenland in the period 2003–2005, using GRACE KBRR (K-Band Ranging Rate) data instead of harmonic coefficients, obtaining higher spatial and temporal resolution. Their estimated value of -101 ± 16 Gt yr^{-1} is substantially smaller than that obtained from Velicogna & Wahr (2006b) and Chen *et al.* (2006b). They suggest that the main difference lies in the different spatial resolution that does not allow to reproduce the correct spatial pattern in customary level 2 data treatment. This is certainly true, and suggests that the techniques employed to overcome this limitation are crucial: even sophisticated methods can produce corrections in the wrong direction if they do not reflect the local features of the area and phenomena under examination.

On the other hand, the comparison with estimates based on non-gravitational data, for example, altimetric surveys and on glacier dynamics arguments, is not trivial. Most of the works agree in giving a substantial mass loss both in Greenland and Antarctica, but their quantitative estimates can be very different. As pointed out in the previous work of Zwally *et al.* (2005), these methods are subject to potentially large uncertainties, due to the limited time span of the altimetric campaigns as well as to their uncomplete spatial coverage of the regions where ice mass changes occur, both requiring further extrapolations. But the main problem is probably the very difficult inclusion of the firn compaction effects in these estimates. Indeed while GRACE data, though with limited resolution, measure directly mass variations, these methods derive mass from volume variations. Local warming in fact produces melting of ice sheets, and so a mass reduction, but also firn compaction, that instead produces volume reduction without net mass loss. Both these phenomena, however, produce a volume reduction, and so differences in the firn compaction treatments can give substantially different mass variations estimates.

Moreover, warming may cause melting in the outer regions but accumulation in the inner regions due to increased precipitations, and so the net balance can be non-trivial. Furthermore, the change in the morphological distribution of ice produces steep ice surfaces in the outer regions, that, for example, are not accurately measured in altimetric surveys. For these reasons, even non-gravitational mass variations estimates can be affected by substantial uncertainties, mainly in smaller areas, as in the Greenland case. This can be at the origin of the rather wide variety of results available in literature, and thus one can find estimates based on altimetric surveys and on glacier dynamics arguments in Greenland (Rignot *et al.* 2006) that substantially agree with the GRACE based estimates of Velicogna & Wahr (2006b) and Chen *et al.* (2006b), but other works which give very different results: Zwally *et al.* (2005) provide for the period 1992–2002 a small mass gain in Greenland ($+11 \pm 3$ Gt yr^{-1}), and most of all show that differences in the altimetric data analysis can affect strongly the estimates.

For these reasons, a really accurate determination of mass variations is still far from being available, both on gravitational and altimetric-glaciological basis, though in the future the availability of time-series spanning a larger interval will make GRACE based estimates more reliable and accurate.

5 CONCLUSIONS

In this work, we provide realistic bounds to the estimates of ice mass changes in Antarctica and Greenland based on the level 2 data from GRACE mission. We developed and applied our own analysis to the gravitational time-series available from 2003 January to 2006 April to obtain mass trends over the two regions, and also computed the same quantity employing the mass grids provided by Chambers (Chambers 2006), for the same time interval. We made use of some simple techniques to account for the limited spatial resolution and the related edge effects, but we purposely chose a simplified approach to avoid that the differences in the treatment of physical signals could be disguised by processing subtleties. The results obtained are in substantial agreement with most of the recently published works based on GRACE data, but we show that the results are affected by larger uncertainties than commonly stated. Gravitational variations allow one in principle to directly measure mass variations, so does the GRACE time-series. However, the limited time interval spanned by the mission data makes the estimates of secular trends a difficult task, and this mainly holds for the earlier releases. Moreover, the techniques employed by the three main analysis centres to produce the level 2 data are constantly improving and, as we show, the results obtained from different releases can vary significantly (up to 24 per cent in Antarctica).

Most importantly, we accurately take into account the effect of variations in the solid Earth parameters and in the isostatic adjustment after Pleistocene deglaciation process on the present-day ice mass variations estimates.

A thorough search in the upper–lower-mantle viscosity space for PGR contribution and the use of our own data treatment together with that carried out by Chambers for GFZ R03, allows us to obtain a wide, and realistic, interval for present-day mass variations in Antarctica and Greenland. We obtained an ice loss of -209 Gt yr^{-1}, by combining our stiff lower mantle PGR model with our own estimate of linear mass trend over Antarctica, and an ice accumulation of 88 Gt yr^{-1}, by subtracting our soft lower mantle PGR model from the linear trend obtained from Chambers mass grids (GFZ R03).

Greenland, instead, is loosing mass at a rate between −122 and −50 Gt yr^{-1}.

We believe that these bounds are more realistic than those that have appeared in the literature, since we explore a wider spectrum of viscosity values, jointly with mass trends intervals estimated from various data treatment approaches. Considering the PGR contribution for the most probable lower mantle viscosity of 10^{22} Pa s, in agreement with mantle viscosities from geoid anomalies driven by mantle convection, we obtain an ice loss in Antarctica and Greenland that, within the range of variability, is in full agreement with previous SLR estimates from a longer time-series of 20 yr of long wavelength zonal components of the gravity field, based on a rigorous inversion scheme to extract the preferred mantle viscosity of 10^{22} Pa s.

This agreement of course makes our GRACE estimates for mass trends robust, being in accord with a totally different technique and methodology to extract the linear trends in the gravity data.

Our study confirms the trend of a substantial ice mass loss both in Greenland and Antarctica, also in agreement with other recent works based on gravitational, altimetric and glacier dynamics surveys.

Even when using gravitational data, a definite quantitative accurate estimate, however, is not available, and improvement in the data processing techniques, as well as a better knowledge of solid Earth parameters, of deglaciation processes, together with the availability of data spanning longer time interval, or derived from future space mission, will certainly help in reducing the present uncertainties.

ACKNOWLEDGMENTS

GRACE data were processed by D. P. Chambers, supported by the NASA Earth Science REASoN GRACE Project, and are available at http://grace.jpl.nasa.gov. This work is supported by the GOCE-Italy project of the Italian Space Agency (ASI). We are indebted to the anonymous reviewers for their important suggestions. We thank Jerry Mitrovica for important discussion.

REFERENCES

Bettadpur, S., 2003. Level-2 gravity field product user handbook, GRACE Proj., Univ. of Tex., Austin.

Bettadpur, S., Flechtner, F. & Schmidt, R., 2006. Technical Note 04: Usage Guidelines for GFZ RL03 and JPL RL02 GRACE Gravity Fields & Atmosphere/Ocean Background Models, GRACE Proj., Univ. of Tex., Austin.

Chambers, D.P., 2006. Evaluation of new GRACE time-variable gravity data over the ocean, *Geophys. Res. Lett.,* **33,** L17603, doi:10.1029/2006GL027296.

Chen, J.L., Wilson, C.R., Famiglietti, J.S. & Rodell, M., 2005. Spatial sensitivity of the Gravity Recovery and Climate Experiment (GRACE) time-variable gravity observations, *J. geophys. Res.,* **110,** B08408, doi:10.1029/2004JB003536.

Chen, J.L., Wilson, C.R. & Tapley, B.D., 2006a. Satellite gravity measurements confirm accelerated Melting of Greenland Ice sheet, *Science,* **313,** 1958, doi:10.1126/science.1129007.

Chen, J.L., Wilson, C.R., Blankenship, D.D. & Tapley, B.D., 2006b. Antarctic mass rates from GRACE, *Geophys. Res. Lett.,* **33,** L11502, doi:10.1029/2006GL026369.

Dziewonski, A.M. & Anderson, D.L., 1981. Preliminary reference Earth model, *Phys. Earth planet Inter.,* **25,** 297–356, doi:10.1016/0031-9201(81)90046-7.

Lutchke, S.B. *et al.,* 2006. Recent Greenland Ice mass loss by drainage system from satellite gravity observations, *Science,* **314,** 1286–1289, doi:10.1126/science.1130776.

Mitrovica, J.X. & Forte, A.M., 2004. A new inference of mantle viscosity based upon joint inversion of convection and glacial isostatic adjustment data, *Earth planet. Sci. Lett.,* **225,** 177–189, doi:10.1016/j.epsl.2004.06.005.

Mitrovica, J.X. & Peltier, W.R., 1991. On postglacial geoid subsidence over the equatorial oceans, *J. geophys. Res.,* **96,** 20 053–20 071.

Ramillien, G., Lombard, A., Cazenave, A., Ivins, E.R., Llubes, M., Remy, F. & Biancale, R., 2006. Interannual variations of mass balance of the Antarctica and Greenland ice sheets from GRACE, *Global Plan. Change,* **53,** 198, doi:10.1016/gloplacha.2006.06.003.

Rignot, E. & Kanagaratnam, P., 2006. Changes in the velocity structure of the Greenland ice sheet, *Science,* **311,** 986, doi:10.1126/science.1121381.

Sabadini, R., Yuen, D.A. & Boschi, E., 1982. Polar wandering and the forced responses of a rotating, multilayered, viscoelastic planet, *Geophys. Res.,* **87,** 2885–2903.

Swenson, S. & Wahr, J., 2002. Methods for inferring regional surface-mass anomalies from Gravity Recovery and Climate Experiment (GRACE) measurements of time-variable gravity, *J. geophys. Res.,* **107,** B9,2193, doi:10.1029/2001JB000576.

Swenson, S. & Wahr, J., 2006. Post-processing removal of correlated errors in GRACE data, *Geophys. Res. Lett.,* **33,** L08402, doi:10.1029/2005GL025285.

Tamisiea, M.E., Leuliette, E.W., Davis, J.L. & Mitrovica, J.X., 2005. Constraining hydrological and cryospheric mass flux in southeastern Alaska using space-based gravity measurements, *Geophys. Res. Lett.,* **32,** L20501, doi:10.1029/2005GL023961.

Tosi, N., Sabadini, R., Marotta, A.M. & Vermeersen, L.L.A., 2005. Simultaneous inversion for the Earth's mantle viscosity and ice mass imbalance in Antarctica and Greenland, *J. geophys. Res.,* **110,** B07402, doi: 10.1029/2004JB003236.

Tushingham, A.M. & Peltier, W.R., 1991. Ice-3G: a new global model of late Pleistocene Deglaciation Based upon Geophysical prediction of Post-Glacial Relative Sea Level Change, *J. geophys. Res.,* **96**(B3), 4497–4523.

Velicogna, I. & Wahr, J., 2005. Greenland mass balance from GRACE, *Geophys. Res. Lett.,* **32,** L18505, doi:10.1029/2005GL023955.

Velicogna, I. & Wahr, J., 2006a. Measurement of time-variable gravity show mass loss in Antarctica, *Science,* **311,** 1754, doi:10.1126/science.1123785.

Velicogna, I. & Wahr, J., 2006b. Acceleration of Greenland ice mass loss in spring 2004, *Nature,* **443,** 21, 329, doi:10.1038/nature.05168.

Wahr, J., Molenaar, M. & Bryan, F., 1998. Time variability of the Earth's gravity field: Hydrological and oceanic effects and their possible detection using GRACE, *J. geophys. Res.,* **103**(B12), 30 205–30 229.

Wahr, J., Swenson, S., Zlotnicki, V. & Velicogna, I., 2004. Time-variable gravity from GRACE: first results, *Geophys. Res. Lett.,* **31,** L11501, doi:10.1029/2004GL019779.

Zwally, H.J., Giovinetto, M.B., Li, J., Cornejo, H.G., Beckley, M.A., Brenner, A.C., Saba, J.L. & Yi, D., 2005. Mass changes of the Greenland and Antarctic ice sheets and shelves and contributions to sea-level rise: 1992–2002, *J. Glaciol.,* **51,** 509.